PAPER

High aspect ratio silicon nanowires control fibroblast adhesion and cytoskeleton organization

To cite this article: Laura Andolfi *et al* 2017 *Nanotechnology* **28** 155102

IOP Publishing Nanotechnology
Nanotechnology **28** (2017) 155102 (9pp) https://doi.org/10.1088/1361-6528/aa5f3a

High aspect ratio silicon nanowires control fibroblast adhesion and cytoskeleton organization

Laura Andolfi[1], Anna Murello[1,4], Damiano Cassese[1,5], Jelena Ban[2,3], Simone Dal Zilio[1] and Marco Lazzarino[1]

[1] Istituto Officina dei Materiali, Consiglio Nazionale delle Ricerche (IOM-CNR) Basovizza, Area Science Park, I-34149 Trieste, Italy
[2] International School for Advanced Studies (SISSA), Via Bonomea, 265, I-34136 Trieste, Italy
[3] Department of Biotechnology, University of Rijeka, Radmile Matejčić 2, 51000 Rijeka, Croatia

E-mail: andolfi@iom.cnr.it

Received 22 November 2016, revised 2 February 2017
Accepted for publication 7 February 2017
Published 17 March 2017

Abstract

Cell–cell and cell–matrix interactions are essential to the survival and proliferation of most cells, and are responsible for triggering a wide range of biochemical pathways. More recently, the biomechanical role of those interactions was highlighted, showing, for instance, that adhesion forces are essential for cytoskeleton organization. Silicon nanowires (Si NWs) with their small size, high aspect ratio and anisotropic mechanical response represent a useful model to investigate the forces involved in the adhesion processes and their role in cellular development. In this work we explored and quantified, by single cell force spectroscopy (SCFS), the interaction of mouse embryonic fibroblasts with a flexible forest of Si NWs. We observed that the cell adhesion forces are comparable to those found on collagen and bare glass coverslip, analogously the membrane tether extraction forces are similar to that on collagen but stronger than that on bare flat glass. Cell survival did not depend significantly on the substrate, although a reduced proliferation after 36 h was observed. On the contrary both cell morphology and cytoskeleton organization revealed striking differences. The cell morphology on Si-NW was characterized by a large number of filopodia and a significant decrease of the cell mobility. The cytoskeleton organization was characterized by the absence of actin fibers, which were instead dominant on collagen and flat glass support. Such findings suggest that the mechanical properties of disordered Si NWs, and in particular their strong asymmetry, play a major role in the adhesion, morphology and cytoskeleton organization processes. Indeed, while adhesion measurements by SCFS provide out-of-plane forces values consistent with those measured on conventional substrates, weaker in-plane forces hinder proper cytoskeleton organization and migration processes.

Supplementary material for this article is available online

Keywords: silicon nanowires, mechanotransduction, adhesion, single cell force spectroscopy

(Some figures may appear in colour only in the online journal)

Introduction

Cell adhesion is a complex biological process that plays a central role in regulating a large variety of fundamental physiological and pathological cellular activities such as

[4] Present address: Ecole Polytechnique Fédérale de Lausanne (EPFL), CH-1015 Lausanne, Switzerland.
[5] Present address: Ape Research, Srl, AREA Science Park, Basovizza, Trieste, Italy.

migration, proliferation, differentiation, metastasis, immunological response, communication development and maintenance of tissues [1–3]. When cells adhere to a substrate they extend explorative elongation structures to sense the chemical or physical cues of the extracellular environment. Subsequently, this adhesion process is mediated by integrin transmembrane receptors that bind to the extracellular environment and recall a network of cytoplasmic proteins that ensure connection and communication with cytoskeleton actin fibres [3].

This forms the basis of focal adhesion sites, a dynamic machinery that rapidly assembles and disassembles during cell migration, able to tune a number of signalling pathways that mediate cell adhesion and migration [3–5] and consequently proliferation and survival. Indeed, when cells are cultured under conditions that prevent adhesion and spreading, they stop growing and lose viability [6].

Although cell adhesion has been widely investigated and several biochemical pathways elucidated, some issues still have to be clarified about the forces involved in the cellular response to the geometrical and mechanical properties of the environment and how this cellular response evolves over time. For such an aim nanostructured supports are very useful to investigate how different geometry and/or elasticity affect cell adhesion, migration, growth and differentiation [7–9]. Among nanostructured supports, nanowires have attracted attention because of their nanometric size, high aspect ratio and a broad range of mechanical, optical and electrical features [10, 11]. Such characteristics make them highly suitable as versatile platform for cell manipulation [12], biosensors [10, 13] drug delivery [14] and study of the forces exerted on and/or by the cells upon adhesion and migration [15, 16]. This last issue is of particular importance for clarifying the mechanotransduction mechanisms that convert external mechanical stimuli into biological response and allows for interfacing the cell with the external environment (i.e. extracellular matrix, neighbouring cells or artificially engineered material). Kim *et al* reported on the spontaneous penetration of vertical NWs in the cell membrane thus affecting cell viability [17]; on the other hand Shalek *et al* obtained NWs penetration without affecting cell viability and thus enabling microinjection and release of various reagents into the cell [14].

Persson *et al* cultured fibroblasts on non-ordered vertically arrays of GaP NWs, observing no plasma membrane penetration, but reduced cell mobility and proliferation [18]. Similarly InAs-NWs are observed to affect morphology, adhesion and cell viability of an embryonic kidney cell [10].

Finally, small tuning of NW characteristics in terms of length, diameter, density and elasticity can promote a specific cell lineage differentiation toward chondrocytes [19] and osteocytes [19, 20] and neural lineage [21] without the presence of specific induction proteins in the medium, thus evidencing the relevant potential of NWs to trigger a biological reaction.

However, up to now, a detailed investigation and quantification of the forces developed in the interaction of cells with nanostructures and their relation with cytoskeleton organization is still missing.

In this work the interaction of mouse embryonic fibroblasts (MEFs) with substrates densely covered by high aspect ratio flexible silicon nanowires (Si NWs) is investigated. The adhesion forces between MEF and Si-NWs, collagen and bare glass substrates were measured and quantified by single cell force spectroscopy (SCFS). This technique enables measuring the adhesion strength with force sensitivity in the pN range and temporal resolution of the order of a few seconds while standard cell adhesion assays require long time periods (from a few minutes up to hours) [22–26]. The morphology, cytoskeleton organization and MEF's ability to spread on Si-NWs after culturing are analyzed by scanning electron (SEM) and confocal fluorescence microscopy. The proliferation rate on Si-NWs support was also investigated.

Materials and methods

Si NWs fabrication

Silicon nanowires were grown on a glass coverslip in a PECVD reactor, using Au as a catalyst and SiH_4 as a precursor. The growth time was used to control the NWs length, while keeping catalyst and NW density constant. For relatively short growing times the NW film is mainly composed of short NWs that densely cover the substrate with the presence of a few longer ones; this is due to the non homogeneous diffusion limited growth process in which thin NW grow faster. However by increasing the growth time the growth of the thin NWs is limited by substrate-to-tip diffusion, and eventually all NWs have the same length.

Cell culture and proliferation analysis

Primary mouse embryonic fibroblasts (MEFs) were prepared from C56/BL mice as described in [27] and cultured in DMEM supplemented with 15% fetal bovine serum and 1% antibiotics penicillin/streptomycin (Thermo Fisher Scientific, Waltham, MA, USA) at 37 °C, 5% CO_2. In order to evaluate cell proliferation, approximately 20 000 cells were seeded on Si-NWs, collagen coated and bare glass coverslip. A coating on glass coverslip was achieved with 0, 1% gelatin (Sigma-Aldrich) in phosphate-buffered saline (PBS) for 15 min at room temperature and subsequent washing with PBS. In this work we refer to this type of coating as collagen-coated samples. Cell density was evaluated at 12, 24 and 36 h from cell seeding. Specifically, each time sample was washed twice with PBS and fixed with 4% paraformaldehyde (Sigma-Aldrich) for 20 min, then washed with PBS and incubated with DAPI for nuclei staining, then used for cell counting. Afterwards, phase contrast images and DAPI-positive cells were taken by Axiovert 200 inverted microscope (Carl Zeiss, Jena, Germany) (10X objective).

Scanning electron microscopy

After 12 h, the culturing medium was aspirated and samples were fixed as described above. Afterward they were dehydrated using a series of ethanol steps with increasing

concentration from 50% to 90% ethanol for 5 min each and by a critical-point drying procedure. Then sample were sputtered-coated with a thin layer of Au (thickness of approximately 10 nm). A low current and bias have been employed for the deposition process to reduce the damage of the cell. Imaging was performed at low acceleration voltage (2 keV) by detecting secondary electrons in planar and 45° tilted configuration in a Zeiss Supra40 SEM.

Focused ion beam milling

A rough milling at 20–100 pA current and 30 KV was performed using a Ga+ ion beam (LEO 1540 crossbeam) to create a groove in the selected cell. After lowering ion beam current and voltage, the resulting groove was observed by standard SEM imaging (voltage 3 KV, working distance 5 mm, tilt angle 54°, current 50 pA) with a ZEISS in lens detector to better highlight the morphology of the cell section and increase the contrast for different materials.

Immunostaining and confocal microscopy

Cells were fixed in 4% paraformaldehyde containing 0.15% picric acid in PBS, saturated with 0.1 M glycine, permeabilized with 0.1% Triton X-100, saturated with 0.5% BSA (Sigma-Aldrich) in PBS and then incubated for 1 h with rabbit polyclonal anti-fibronectin antibody (Merck Millipore, Darmstadt, Germany). The secondary antibody was goat anti-rabbit Alexa Fluor® 594, F-actin was marked with Alexa Fluor® 488 phalloidin (Thermo Fisher Scientific) and the incubation time was 30 min. Nuclei were stained with 2 μg ml^{-1} in PBS Hoechst 33342 (Sigma-Aldrich) for 5 min. All the incubations were performed at room temperature (20 °C–22 °C). The cells were examined using a Leica DMIRE2 confocal microscope (Leica Microsystems GmbH, Wetzlar, Germany) equipped with DIC and fluorescence optics, diode laser 405 nm, Ar/ArKr 488 nm and He/Ne 543/594 nm lasers. 63× magnification and a 1.4 NA objective was used. Images were acquired at 1024 × 1024 pixels resolution and z stacks with 200–250 nm step size. Image processing was performed Image J by W Rasband (developed at the US National Institutes of Health and available at http://rsbweb.nih.gov/ij/).

Single cell force spectroscopy set-up and adhesion measurements

SCFS measurements were carried out by a NanoWizard atomic force microscope (AFM) (JPK Instruments, Berlin, Germany) mounted on top of an Axiovert 200 inverted microscope (Carl Zeiss, Jena, Germany) with a CellHesion module that enables extention of the vertical range of AFM from 15 μm up to 100 μm thus enabling complete cell detachment from substrate. All experiments were performed at 37 °C using a temperature-controlled BioCell chamber (JPK Instruments, Berlin, Germany). MEF cultured on a collagen (Sigma-Aldrich) coated petri dish, were detached from the petri dishes by incubating cells for 10 min with 0.5% trypsin–EDTA (Thermo Fisher Scientific), re-suspended in culture medium and then inserted into the BioCell about 20 min after removal from a petri dish. Adhesion measurements were performed using tipless V-shaped silicon nitride cantilevers having a nominal spring constant of 0.32 N m^{-1} or 0.08 N m^{-1} (NanoWorld, Innovative Technologies). O_2 plasma treated cantilevers were functionalized with concanavalin-A (Sigma-Aldrich) (incubation 10 μM for 15 h at 4 °C) and stored in PBS. Before each experiment the cantilever spring constant was calibrated by using the thermal noise method [28]. In order to allow MEF cell binding to the cantilever the NWs support were grown only on half of the glass coverslip while the resting half was coated with bovine serum albumin (BSA), for which MEF cells have low affinity. Once the cells are inserted into the chamber the concanavalin-A functionalized cantilever is pressed on a single a cell against the BSA layer for 30 s with a contact force of 0.7–1 nN to allow a stable immobilization of the cell. Then the cell was lifted from the surface and allowed to establish a firm adhesion to the cantilever for about 15 min. Afterwards the cantilever was moved toward the NWs area and adhesion measurements were performed at a contact force of 0.5 nN for different contact times (10, 20, 40, 80 and 160 s) in the culture medium. After each force measurement, the cell was retracted to recover for a period of time slightly higher than the contact time with the surface, before adhering to a different spot on the surface. An optical microscope was used to monitor the cell status during the measurements, which were interrupted as soon as changes in cell morphology was observed. During contact, the piezo height was kept constant using the AFM closed loop feedback mode. The cantilever was withdrawn at constant speed of 5 μm/sec over pulling ranges of 100 μm to ensure complete detachment of the cell from substrate.

Results and discussion

We used substrates densely covered by flexible Si-NWs (figure 1), in order to match the NW mechanical properties with the typical biological forces involved in focal adhesion formation. A characterization of Si NWs used including a distribution of diameter, length, horizontal and vertical projections is reported in the supplementary data (figure S1 is available at stacks.iop.org/NANO/28/155102/mmedia). These Si NWs, 3 ± 1 μm long and 73 ± 20 nm diameter, have an elastic constant in the 0.2–24 mN m^{-1} range. Cells, when migrated can displace focal adhesion points at a rate up to 250 nm min^{-1} [29] and a force larger than 56 pN is required to trigger the formation of focal adhesion points [30]. Thus the nanowires described above which produce forces in the 20–2400 pN range upon displacements of 100 nm are the ideal substrate to investigate the effect of the substrate mechanics on mechanostransduction processes.

The adhesion forces of MEF cells on Si NWs on short-scale time and with pN resolution is measured by SCFS. Representative retraction force traces of MEF on the different supports are shown in figures 2(a)–(c), together with an optical image of a cell attached to the cantilever (figure 2(d)). During the measurements the status of the cell attached to the

Figure 1. SEM micrograph of a Si NW support where the presence of NWs with different lengths can be observed. Stage tilting 54°. Scale bar 1 μm.

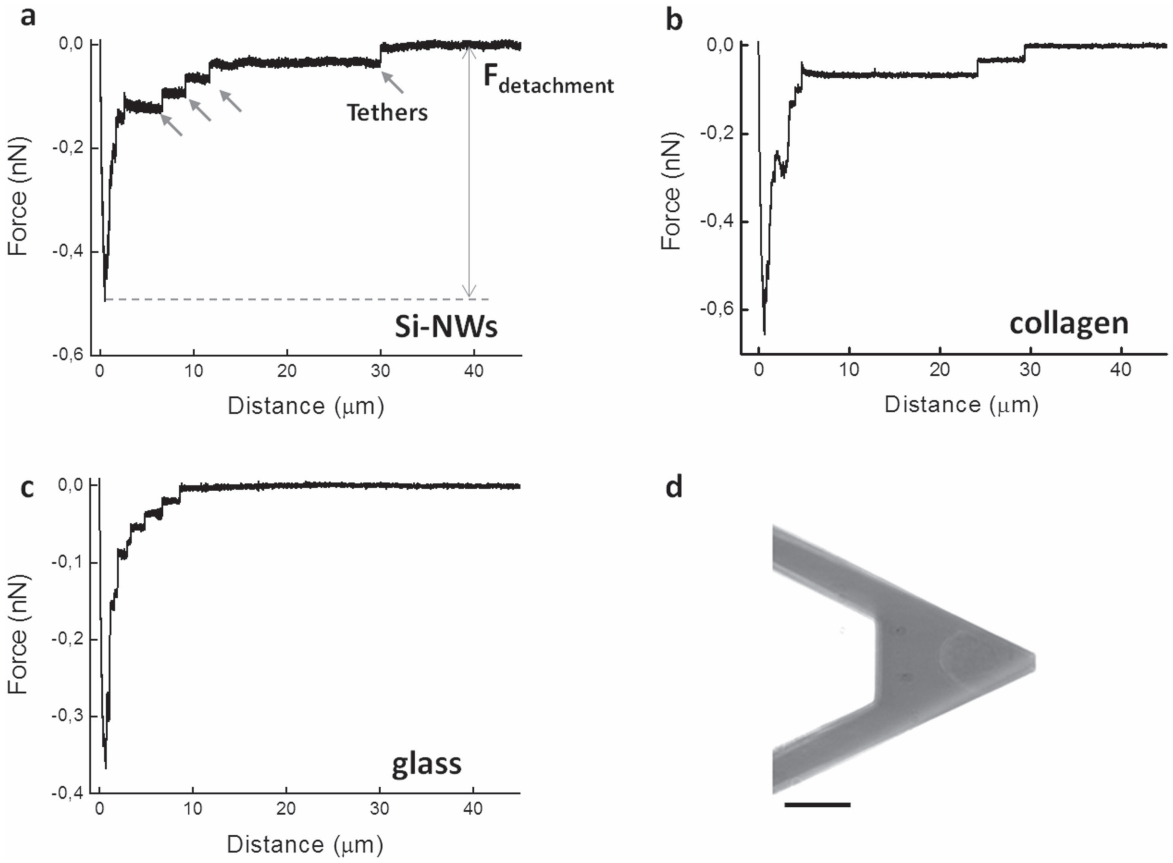

Figure 2. Representative force–distance retraction traces for MEFs on Si NWs (a) on collagen (b) and on glass (c) at 10 s contact time; some features of the curves that enables to quantify adhesion properties as the maximum force exerted for cell detachment and the tether force are indicated by arrows; (d) differential interference contrast optical image of a MEF cell immobilized on a tipless cantilever (scale bar 20 μm).

cantilever did not show significant morphological variations, and the life time of the cell on Si NWs is observed to be comparable to that on collagen and glass coverslip. On the contrary, similar measurements performed on ZnSe NWs grown at low temperature on ITO substrates (online supplementary figure S2) [31] reveal that after a few contacts, the cell forms globular structures related to cell injury and death, with a fast reduction of adhesion forces (online supplementary figures S3 and S4). The same behavior is observed on flat ZnSe substrates and we conclude that the effect arises from ZnSe toxicity rather than a topographical effect. The comparison of the results on ZnSe and Si NWs suggests that the mechanical damage induced during the SCFS measurement, if any, is negligible.

The larger recorded negative value of the force ($F_{\text{detachment}}$) is generally used as a rough measure of the adhesion force; this value is obtained at the beginning of the retraction, when the cell starts to detach from the substrate. Alternatively the energy involved in the adhesion can be obtained by the work of detachment evaluated by integrating the whole area under the force–distance curve. Both focal adhesion points and individual receptors contribute to adhesion force and energy. During further retraction of the cantilever a train of steps is generated by pulling individual

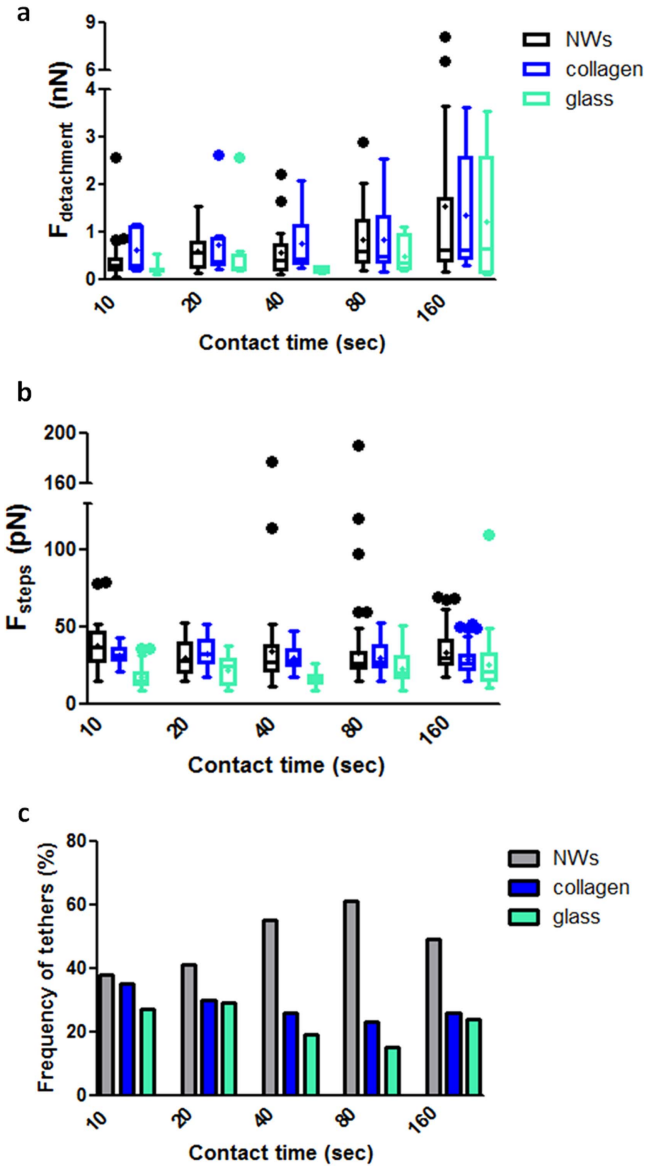

Figure 3. Distributions of the detachment forces obtained for MEF on the three different supports at increasing contact time, in a box-and-whisker plot representation: the values inside the box are the first (25%) and third quartile (75%), the line within the box is the median value (50%), the (−) indicate maximum and minimum of the distribution; while outliers are indicated by (•); the mean value is indicated as (+) (a). The group of data at each contact time are statistically analysed with the Kruskal–Wallis test and Dunn post test to compare all pairs of column. For 10 seconds $p = 0.0557$; for 20 seconds $p = 0.2728$; 40 seconds $p = 0.0423$; 80 seconds $p = 0.5058$; 160 seconds $p = 0.6595$. A set of > 4 curves was acquired for each cell ($n = 3$) on the different supports for each contact time. Tether force distributions for the three supports investigated at increasing contact time (b). The group of data at each contact time are statistically analysed with the Kruskal–Wallis test and Dunn post test. For 10, 20, 40, 80 s the distribution of tether strength on Si NWs is not significantly different from that on collagen, while that on glass is significantly lower than that on Si NWs and collagen ($p < 0.0001$); for 160 s the tether strength on Si NWs and collagen does not significantly differ as well as that of collagen as compared to glass, while the strength on Si NWs is still significantly higher than that on glass ($p < 0.0001$). p value < 0.05 is considered statistically significant. Relative percentage of tethers number observed on the three supports at increasing contact time (c).

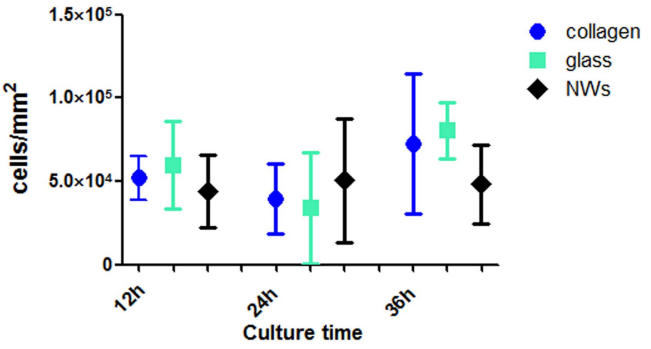

Figure 4. Cell density as function of culture time for MEF cells on Si NWs, collagen and glass coverslip. The density was determined by optical microscope (mean value ± SD).

receptors anchored to the cytoskeleton, which is responsible for the observed elastic response (jumps). Finally long plateaus are observed when the receptors are detached from the cytoskeleton and a membrane nanotube is pulled out the cell body (tether): here the membrane viscosity is mainly responsible for the measured force which depends only on the pulling speed. Jumps and tethers are mainly generated by membrane receptors [32–36]. The results of the detachment force analysis are shown in figure 3(a). The adhesion strength of MEFs on Si NWs is comparable to that observed on collagen for all the time intervals considered, while higher than that obtained on glass, although not significantly different. To analyze in detail the substrate–cell interaction at a single receptor level, we evaluated the force and number of the membrane tethers, by estimating the force steps of the long plateau in the force–distance retraction curve (figure 3(b)). For all contact times, the tether adhesion values of MEF on Si NWs is comparable with those on collagen and significantly higher than those observed on bare flat glass, with a mean value of 30 pN on collagen and Si NWs, while is 20 pN on glass for all interval times. This force appears to be higher on collagen than that observed on glass up to 80 s contact time, while at 160 s contact time they do not significantly differ anymore. This is in agreement with previous works in which a strong attachment of the cells on Si NWs and InAs NWs with respect to a flat substrate of the same materials was estimated by rinsing and centrifugation methods [37, 38]. Moreover MEF cells show a number of tether steps on Si NWs that increases with contact times as compared to glass and collagen coated support (figure 3(c)). Thus MEFs adhere on Si NWs with a high number of interactions having a binding force comparable to that shown on collagen. In general, MEFs are able to develop strong interactions with flexible Si NWs coated glasses, which can represent an interesting alternative to traditional protein coated glasses. Therefore we investigate the effect of such Si NWs on cell proliferation and migration.

In order to assess the effect of the substrate morphology on cellular proliferation, the number of cells was evaluated after 12, 24 and 36 h culture time. After 12 h and 24 h culturing, the cells adhere and proliferate on Si NWs similarly to collagen and glass, while at 36 h the proliferation seems to decrease on Si NWs, but the difference remains within the

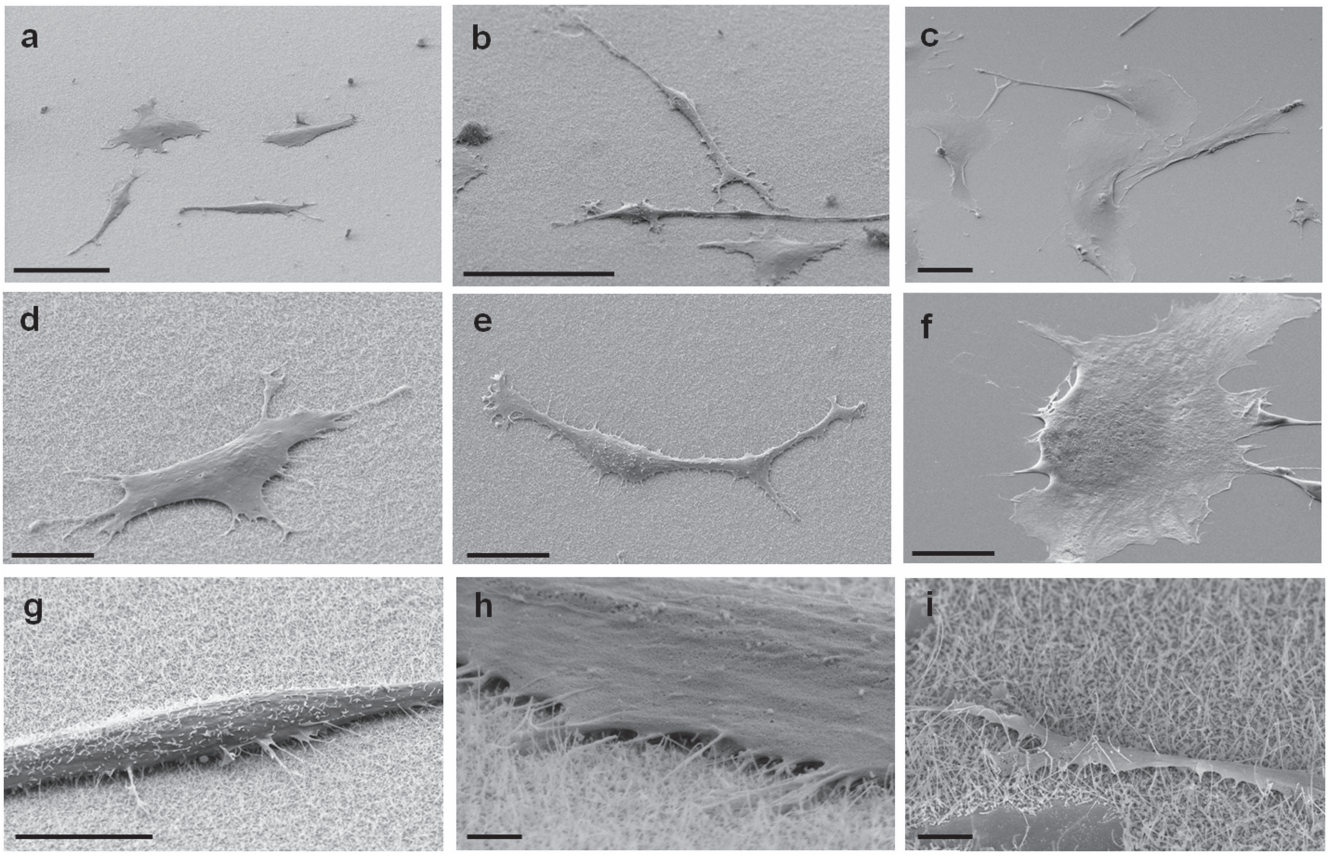

Figure 5. SEM micrographs of MEFs after 12 h culturing on Si NWs (a), (b); (d), (e); (g), (h) and on flat glass support (c), (f), (a)–(c) scale bar 50 μm and (d)–(f) scale bar 10 μm); higher magnification micrographs of MEFs on Si NWs that highlight the presence of numerous filopodia on Si NWs (g scale bare 10 μm) (h scale bar 1 μm) (i scale bar 2 μm).

statistical error (figure 4). From these measurements we can conclude that these Si NWs supports do not affect significantly the short term cellular viability. On the other hand, for longer culture times (96 h), on ordered GaP NWs array a significant lower cell proliferation for fibroblasts was observed, with a stronger effect on longer and denser nanowires substrates [18, 39]. In both cases this behavior seems to be associated also with the formation of multinuclear cells, which were not observed in our short term cultures.

After 12 h culturing, we observe that MEFs adhere and spread on Si NWs similarly to collagen and glass as shown in SEM images (figure 5). However, MEFs cultured on Si NWs frequently display an elongated morphology (figures 5(a), (b), (d) and (e)) as compared to the flat large cell shape commonly observed on flat support (figures 5(c) and (f)). This observation is supported by the cell aspect ratio that for cells on Si NWs is found to be 8 ± 6 (mean $\pm$ SD), higher than that obtained on collagen (2 ± 1) and glass support (4 ± 3). A closer look shows that MEFs on Si NWs are generally characterized by a large number of thin filopodia that surround the cell body and anchor the cell body to the NWs (figures 5(g), (h)). Consistent variations in morphology are observed for different cell types cultured on NWs [20, 37, 38]. Likewise the postnatal retinal cells cultured on GaP NWs extend subtle radial protrusions from the cell body while on flat GaP they assume a polygonal shape [40].

By performing SEM imaging with a tilted angle, it is observed that cells seem to grow suspended on a Si-NW array (figure 5(d)), only in some cases single NWs piercing the thin cellular lateral extension are observed (figure 5(i)). However, FIB milling of MEF cells on NWs together with SEM visualization points to evidence that single NWs do not seem to penetrate the cell membrane and enter into the cell cytoplasm (figure 6), as also observed in previous studies for fibroblast cultured on vertically aligned GaP NWs, where the membrane surrounds the NWs rather than being pierced [18].

Concerning filopodia, commonly they are known to mediate the early steps of adhesion because their main role is to explore the environment, while they quickly disappear in favor of lamellipodia on a flat surface [41]. More recently it is also demonstrated that fibroblasts spreading on microstructured matrix protein arrays primarily use filopodia to reach new adhesive surfaces. Then at the contact of adhesive surfaces, these structures are stabilized and subsequently nucleate lamellipodia-like extensions that lead to full cell spreading [8]. In our case after 12 h culturing numerous filopodia are still present with very little progression toward lamellipodia structures. Although lamellipodia and filopodia are intimately connected in cell protrusion, filopodia alone cannot drive cell motility [42], indeed they have been observed to be integrated into the lamellipodium as the cell edge advances [43]. Such behavior appears in agreement with

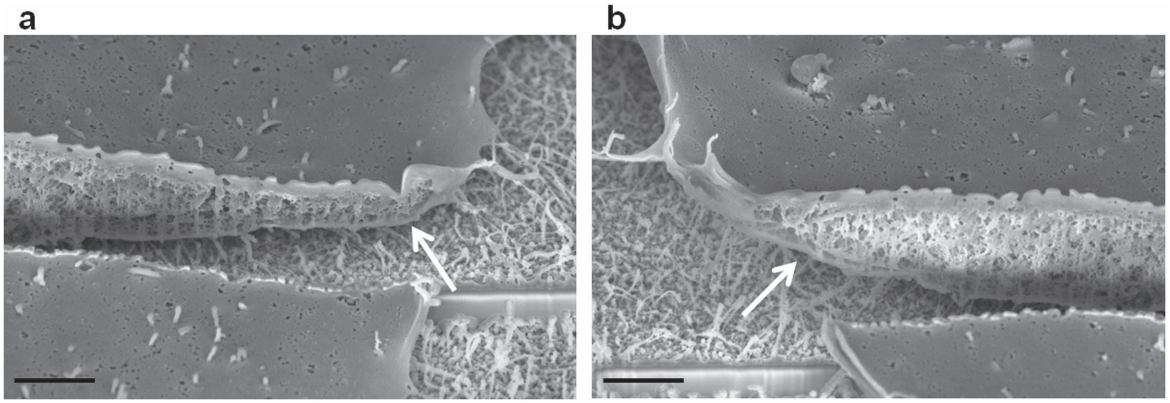

Figure 6. SEM micrographs of FIB milled MEF cells after 12 h culturing on Si NWs. Two lateral side of the groove obtained on single adherent cell are shown in (a) and (b). The white arrows indicate the plasma membrane. Scale bar 1 μm.

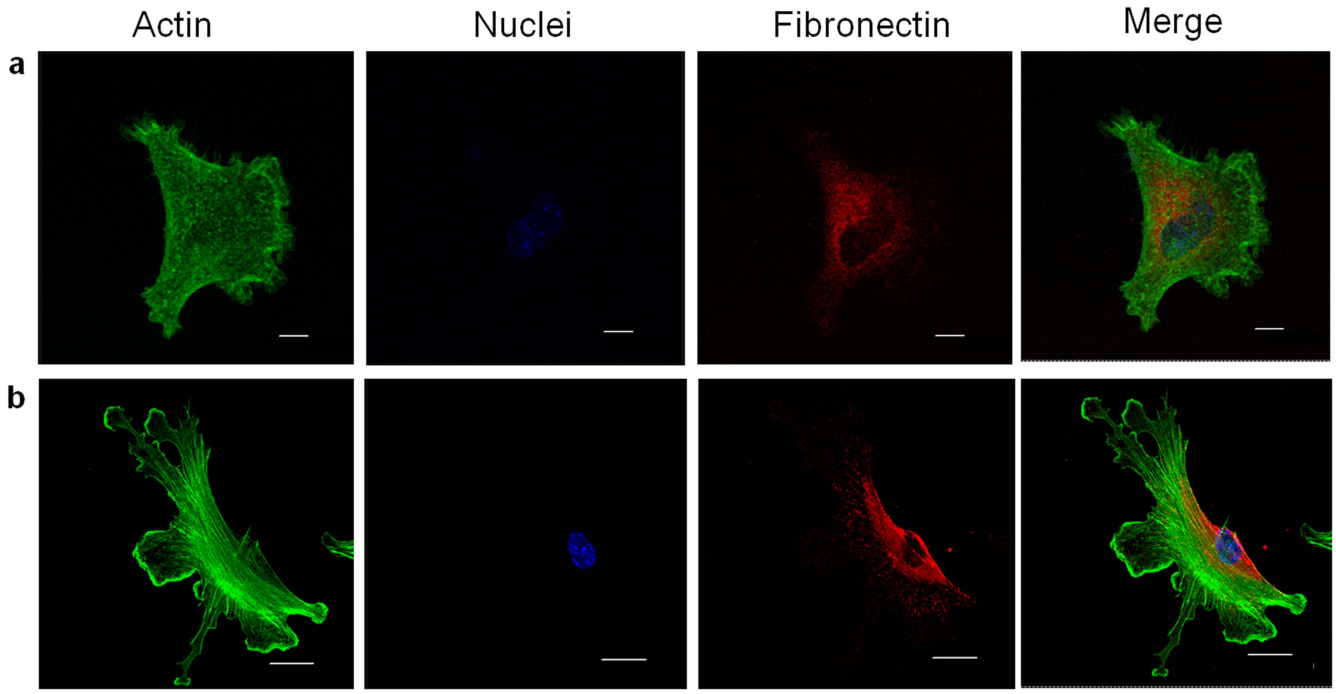

Figure 7. Confocal fluorescence images of MEF cells after 12 h culturing (a) on Si NWs (scale bar 10 μm) and (b) on flat glass substrate (scale bar 25 μm). From left to right: actin in green, fibronectin in red, Hoechst nuclear staining in blue and merge.

what we observed by time-lapse microscopy, where MEFs seem to be trapped on Si NWs with a considerably reduced mobility as compared to that observed on glass or collagen substrate (see movie S1 and movie S2 in the online supplementary data). This decrement in mobility is frequently observed for cells culture on NWs [18, 21, 39]. A more recent work has demonstrated that the reduction in mobility is also related to nanowires density: a lower density remarkably reduces cell mobility and the cell shows long thin protrusions, while in presence of higher density the cell adopts a morphology closer to that on flat control and exhibits a higher mobility [39]. A similar behavior is observed also for neurons that easily attach to pillars that could serve as geometrically superior focal adhesion points for cell attachment, but on the other hand, they markedly reduce the cell mobility by creating a long time trap for neurons [44]. Moreover a lower cell mobility is observed with mesenchymal cells seeded on NWs that showed a preferential neuronal lineage differentiation [21]. Our results and previous works seem to support that the formation of filopodia and long protrusions grasping the Si NWs anchor the cell and reduce its mobility, differently affecting their behavior and fate (i.e. migration, proliferation or differentiation).

The adhesion, spreading and migration are depending on focal adhesion sites formation that occur after a few minutes of contact adhesion, such focal adhesion sites are connected to actin fibers via complex protein interaction. We observed that after 12 h culturing MEF cells on NWs, the actin cytoskeleton organization does not present the well-organized stress fibers (figure 7(a)) typically observed instead on a flat surface (see figure 7(b)). This demonstrates that the NWs support does not allow the fibers formation important for cell

movement, while fibronectin, produced on both NWs and flat support, seems to be distributed according to the actin organization. In general the modifications of cytoplasmic structures organization have been previously observed in response to geometries of the culture support [45].

The absence of well-organized stress fibers has been observed to be guided also by interaction forces generated in the 2D plane. Organization of stress fibers are observed to vary considerably according to the value of surface molecular forces, indeed the actin bundle formation requires molecular tension larger than 56 pN [30]. Indeed the Si NWs substrate can provide large force in the vertical direction, with no significant differences with collagen and glass substrates, as measured by SCFS. However, because of their high flexibility, Si NWs cannot provide large enough in-plane forces. We believe that the lack of enough in-plane rigidity hinders the formation of actin fibers, and therefore cellular migration. Such reduced mobility seems to be a possible responsible of the observed reduction in the proliferation of MEFs on such nanostructures on a longer time scale. Such influence of NWs flexibility on cell behavior is also in agreement with previous studies, where the cell spread and differentiation were correlated with the stiffness of the NWs [20].

Conclusion

Our results suggest that when cells start to adhere in terms of strength, the early exploration process (below 3 min) of cell membrane protrusions is similarly driven by chemical indications (integrin binding with extracellular matrix) as much as by geometry, whereas after some time of adhesion the force in-plane generated by Si-NWs on MEF does not allow them to spread and hinder the formation of actin stress fibers, which determine a considerable reduction of cell mobility. While on flat glass, the cells, independently on chemical interactions, show actin stress fibers and appear free to spread, move and proliferate. These findings indicate that, in the development of the adhesion process, in plane and out of plane forces play a completely different role. They also indicate that more investigations are still required to precisely clarify the role of shape and geometry in mechanostransduction during the adhesion processes which are at the base of cell interaction with biomaterials for devices development for medical applications.

Acknowledgments

L A and M L acknowledge CBM S c r l for providing access to the BioNanoAnalysis core facility. We thank Prof Vincent Torre for useful discussion. We would like to thank Valentina Zannier and Silvia Rubini for providing ZnSe NWs samples. The financial contribution of Area Science Park through the 'open lab' project is kindly acknowledged.

All authors declare no conflict of interest.

References

[1] Manzanares M-V, Webb D J and Horwitz A R 2005 Cell migration at a glance *J. Cell Sci.* **118** 4917–9
[2] Hansen L K, Mooney D J, Vacanti J P and Ingber D E 1994 Integrin binding and cell spreading on extracellular matrix act at different points in the cell cycle to promote hepatocyte growth *Mol. Biol. Cell* **5** 967–75
[3] Huttenlocher A and Horwitz A R 2011 Integrins in cell migration *Cold Spring Harb. Perspect. Biol.* **3** a005074
[4] Hynes R O 1992 Integrins: versatility, modulation, and signaling in cell adhesion *Cell* **69** 11–25
[5] Campbell I D and Humphries M J 2011 Integrin structure, activation and interactions *Cold Spring Harb. Perspect. Biol.* **3** a004994
[6] Meredith J E Jr, Fazeli B and Schwartz M A 1993 The extracellular matrix as a cell survival factor *Mol. Biol. Cell* **4** 953–61
[7] Migliorini E, Ban J, Grenci G, Andolfi L, Pozzato A, Tormen M, Torre V and Lazzarino M 2013 Nanomechanics controls neuronal precursors adhesion and differentiation *Biotechnol. Bioeng.* **110** 2301–10
[8] Guilloua H, Depraz-Deplanda A, Planus E, Vianaya B, Chaussy J, Grichinea A, Albigès-Rizoa C and Blocka M R 2008 Lamellipodia nucleation by filopodia depends on integrin occupancy and downstream Rac1 signaling *Experimental Cell Research* **314** 478–88
[9] Beliveau A, Thomas G, Gond J, Wen Q and Jain A 2016 Aligned nanotopography promotes a migratory state in gliobastoma multiforme tumor cells *Scientific Report* **6** 26143
[10] Bonde S, Buch-Månson N, Rostgaard K R, Andersen T K, Berthing T and Martinez K L 2014 Exploring arrays of vertical one-dimensional nanostructures for cellular investigations *Nanotechnology* **25** 362001
[11] Prinz C N 2015 Interactions between semiconductor nanowires and living cells *J. Phys: Condens. Matter* **27** 233103
[12] Padmanabhan J, Kinser E R, Stalter M A, Duncan-Lewis C, Balestrini J L, Sawyer A J, Schroers J and Kyriakides T R 2014 Engineering cellular response using nanopatterned bulk metallic glass *ACS Nano* **8** 4366–75
[13] Kim D-J, Seol J-K, Lee G, Kim G-S and Lee S-K 2012 Cell adhesion and migration on nanopatterned substrates and their effects on cell-capture yield *Nanotechnology* **23** 395102
[14] Shalek A K *et al* 2010 Vertical silicon nanowires as a universal platform for delivering biomolecules into living cells *Proc. Nat. Acc. Sci.* **107** 1870–5
[15] Albuschies J and Vogel V 2013 The role of filopodia in the recognition of nanotopographies *Sci. Rep.* **3** 1658–68
[16] Hällström W, Lexholm M, Suyatin D B, Hammarin G, Hessman D, Samuelson L, Montelius L, Kanje M and Prinz C N 2010 Fifteen-piconewton force detection from neural growth cones using nanowire arrays *Nano Lett.* **10** 782–7
[17] Kim W, Ng J K, Kunitake M E, Conklin B R and Yang P 2007 Interfacing silicon nanowires with mammalian cells *J. Am. Chem. Soc.* **129** 7228–9
[18] Persson H, Købler C, Mølhave K, Samuelson L, Tegenfeldt J O, Oredsson S and Prinz C N 2013 Fibroblasts cultured on nanowires exhibit low motility, impaired cell division, and DNA damage *Small* **9** 4006–16
[19] Liu D, Yi C, Wang K, Fong C-C, Wang Z, Kwan Lo P, Sun D and Yang M 2013 Reorganization of cytoskeleton and transient activation of Ca2+ channels in mesenchymal stem cells cultured on silicon nanowire arrays *Appl. Mater. Interfaces* **5** 13295−13304

[20] Kuo S W, Lin H I, Hui-Chun Ho J, Shih Y-R V, Chen H-F, Yen T-J and Lee O K 2012 Regulation of the fate of human mesenchymal stem cells by mechanical and stereo-topographical cues provided by silicon nanowires *Biomaterials* **33** 5013–22
[21] Kim H, Kim I, Choi H-J, Kim S Y and Yang E G 2015 Neuron-like differentiation of mesenchymal stem cells on silicon nanowires *Nanoscale* **7** 17131
[22] Tulla M, Helenius J, Jokinen J, Taubenberger A, Müller D J and Heino J 2008 TPA primes a2b1 integrins for cell adhesion *FEBS Letters* **582** 3520–4
[23] Taubenberger A, Cisneros D A, Friedrichs J, Puech P-H, Muller D J and Franz C M 2007 Revealing early steps of 21 integrin-mediated adhesion to collagen type I by using single-cell force spectroscopy *Mol. Biol. Cell* **18** 1634–44
[24] Andolfi L, Bourkoula E, Migliorini E, Palma A, Pucer A, Skrap M, Scoles G, Beltrami A P, Cesselli D and Lazzarino M 2014 Investigation of adhesion and mechanical properties of human glioma cells by single cell force spectroscopy and atomic force microscopy *PLoS One* **9** e112582
[25] Friedrichs J, Legate K R, Schubert R, Bharadwaj M, Werner C, Müller D J and Benoit M 2013 A practical guide to quantify cell adhesion using single-cell force spectroscopy *Methods* **60** 169–78
[26] El-Kirat-Chatel S and Dufrêne Y F 2016 Nanoscale adhesion forces between the fungal pathogen Candida albicans and macrophages *Nanoscale Horiz.* **1** 69–74
[27] Jozefczuk J, Drews K and Adjaye J 2012 Preparation of mouse embryonic fibroblast cells suitable for culturing human embryonic and induced pluripotent stem cells *J. Vis. Exp.* **64** e3854
[28] Te Riet J *et al* 2011 Interlaboratory round robin on cantilever calibration for AFM force spectroscopy *Ultramicroscopy* **111** 1659–69
[29] Burnette D T, Manley S, Sengupta P, Sougrat R, Davidson M W, Kachar B and Lippincott-Schwartz J 2011 A role for actin arcs in the leading-edge advance of migrating cells *Nat. Cell Biol.* **13** 371–82
[30] Wang X and Ha T 2013 Defining single molecular forces required to activate integrin and notch signaling *Science* **340** 991–4
[31] Zannier V, Martelli F, Grillo V, Plaisier J R, Lausi A and Rubini S 2014 Strong blue emission from ZnSe nanowires grown at low temperature *Phys. Status Solidi RRL* **8** 182–6
[32] Müller D J, Helenius J, Alsteens D and Dufrêne Y F 2009 Force probing surfaces of living cells to molecular resolution *Nat. Chem. Biol.* **5** 383–90
[33] Hochmuth R M, Shao J-Y, Dai J and Sheetz M P 1996 Deformation and flow of membrane into tethers extracted from neuronal growth cones *Biophys. J.* **70** 358–69
[34] Baoukina S, Marrink S J and Tieleman D P 2012 Molecular structure of membrane tethers *Biophys. J.* **102** 1866–71
[35] Heinrich V, Leung A and Evans E 2005 Nano- to microscale dynamics of P-selectin detachment from leukocyte interfaces. II. tether flow terminated by P-selectin dissociation from PSGL-1 F *Biophys. J.* **88** 2299–308
[36] Brochard-Wyart F, Borghi N, Cuvelier D and Nassoy P 2006 Hydrodynamic narrowing of tubes extruded from cells *Proc. Natl Acad. Sci.* **103** 7660–3
[37] Bonde S *et al* 2013 Tuning InAs nanowire density for HEK293 cell viability, adhesion, and morphology: perspectives for nanowire-based biosensors *ACS Appl. Mater. Interfaces* **5** 10510–9
[38] Qi S J, Yi C Q, Ji S L, Fong C C and Yang M S 2009 Cell adhesion and spreading behavior on vertically aligned silicon nanowire arrays *ACS Appl. Mater. Interfaces* **1** 30–4
[39] Persson H, Li Z, Tegenfeldt J O, Oredsson S and Prinz C N 2015 From immobilized cells to motile cells on a bed-of-nails: effects of vertical nanowire array density on cell behaviour *Sci. Rep.* **5** 18535
[40] Piret G, Perez M T and Prinz C N 2013 Neurite outgrowth and synaptophysin expression of postnatal CNS neurons on GaP nanowire arrays in long-term retinal cell culture *Biomaterials* **34** 875–87
[41] Davenport R W, Dou P, Rehder V and Kater S B 1993 A sensory role for neuronal growth cone filopodia *Nature* **361** 721–4
[42] Euteneuer U and Schliwa M 1984 Persistent, directional motility of cells and cytoplasmic fragments in the absence of microtubules *Nature* **310** 58–61
[43] Nemethova M, Auinger S and Small J V 2008 Building the actin cytoskeleton: filopodia contribute to the construction of contractile bundles in the lamella *J. Cell Biol.* **180** 1233–44
[44] Xie C, Hanson L, Xie W J, Lin Z L, Cui B X and Cui Y 2010 Non invasive neuron pinning with nanopillar arrays *Nano Lett.* **10** 4020–4
[45] Estévez M, Fernández-Ulibarri I, Martinez E, Egea G and Samitier J 2010 Changes in the internal organization of the cell by microstructured substrates *Soft Matter* **6** 582–90